Biochemical and Biophysical Research Communications 456 (2015) 129–134

Contents lists available at ScienceDirect

Biochemical and Biophysical Research Communications

journal homepage: www.elsevier.com/locate/ybbrc

ABCD2 identifies a subclass of peroxisomes in mouse adipose tissue

Xiaoxi Liu, Jingjing Liu, Joshua D. Lester, Sonja S. Pijut, Gregory A. Graf *

Department of Pharmaceutical Sciences, Saha Cardiovascular Research Center, Barnstable Brown Diabetes and Obesity Center, University of Kentucky, Lexington, KY, United States

ARTICLE INFO

Article history:
Received 4 November 2014
Available online 24 November 2014

Keywords:
Peroxisome
ABC transporter
Adipose tissue
Subcellular organelle
Proteomics

ABSTRACT

ATP-binding cassette transporter D2 (D2) is an ABC half transporter that is thought to promote the transport of very long-chain fatty acyl-CoAs into peroxisomes. Both D2 and peroxisomes increase during adipogenesis. Although peroxisomes are essential to both catabolic and anabolic lipid metabolism, their function, and that of D2, in adipose tissues remain largely unknown. Here, we investigated the D2 localization and the proteome of D2-containing organelles, in adipose tissue. Centrifugation of mouse adipose homogenates generated a fraction enriched with D2, but deficient in peroxisome markers including catalase, PEX19, and ABCD3 (D3). Electron microscopic imaging of this fraction confirmed the presence of D2 protein on an organelle with a dense matrix and a diameter of ~200 nm, the typical structure and size of a microperoxisome. D2 and PEX19 antibodies recognized distinct structures in mouse adipose. Immunoisolation of the D2-containing compartment confirmed the scarcity of PEX19 and proteomic profiling revealed the presence of proteins associated with peroxisome, endoplasmic reticulum (ER), and mitochondria. D2 is localized to a distinct class of peroxisomes that lack many peroxisome proteins, and may associate physically with mitochondria and the ER.

1. Introduction

Peroxisomes were initially identified in kidney and liver cells as a subcellular organelle characterized by a single membrane containing a granular matrix and a crystalline core [1]. These dynamic organelles have been shown present in all mammalian tissues and cells including adipocytes [2–4]. Besides the removal of reactive oxygen species, peroxisomes are also metabolically involved in the β-oxidation of very long chain fatty acids, α-oxidation of branched chain fatty acids, and biosynthesis of ether-phospholipids [2].

Peroxisomes in adipose tissues are often referred to as "microperoxisomes" that dramatically increased in number during differentiation of cultured 3T3-L1 adipocytes and were found in close proximity to lipid droplets [4]. Recently, emerging evidence indicates that peroxisome metabolism critical for normal adipose functioning [5,6]. In Pex7 deficient mice, peroxisome biogenesis is impaired due to the failure of peroxisomal protein import [6]. These mice lack plasmalogens, the synthesis of which strictly relies on peroxisomal metabolism, and had severely reduced adiposity despite similar food intake. In another mouse model in which Pex5 was specifically deleted in adipose using aP2 promoter, peroxisomes were dysfunctional in white adipose tissue, but intact in liver, heart, pancreas, and muscle [5]. Adipose function impairment resulted in reduced lipolysis and increased fat mass. Other phenotypes were also observed, including failure of catalase import into peroxisomes in the nervous system, impaired shivering thermogenesis, and reduced plasma adrenaline levels, suggesting some adipose phenotypes were due to secondary effect or off-target Pex5 deletion.

ABCD2 has been proposed as a peroxisomal ABC transporter that promotes the transport of very long-chain fatty acyl-CoA into peroxisomes for β-oxidation [7]. The D2 protein is expressed in brain, skeletal muscle, lung, liver, and testis, but is most abundant in adipose tissues in mice, and highly expressed in cultured 3T3-L1 adipocytes [8]. D2 deficient adipose tissue showed an increase in the abundance of 20:1 and 22:1 fatty acids. When D2 deficient mice were challenged with dietary erucic acid (C20:1), they exhibited rapid onset of obesity, hepatic steatosis, and insulin resistance [9]. While these data support a key role for D2 in lipid metabolism, the function of D2 in adipose and its relationship to adipose peroxisome metabolism remains unclear.

To determine the subcellular localization of D2 and its relationship to adipose peroxisomes, we isolated D2-containing organelles from mouse adipose tissue using two independent approaches. Our data indicates that the D2-compartment lacks some of the

* Corresponding author at: Pharmaceutical Sciences, University of Kentucky, Room 345 Biopharmaceutical Complex, 789 South Limestone Street, Lexington, KY 40536, United States. Fax: +1 859 257 7564.

E-mail addresses: xiaoxi.liu@uky.edu (X. Liu), jingjing.liu0@gmail.com (J. Liu), joshua.lester@uky.edu (J.D. Lester), srhee2@uky.edu (S.S. Pijut), Gregory.Graf@uky.edu (G.A. Graf).

http://dx.doi.org/10.1016/j.bbrc.2014.11.046
0006-291X/

well-known peroxisomal proteins, such as catalase and PEX19, but possesses other peroxisomal enzymes. These results suggest an association of this organelle with mitochondria and ER. The protein most strongly-associated with D2 was a leucine-rich repeat containing protein 59 (LRRC59), a poorly characterized protein implicated in intracellular trafficking of FGF1 [10].

2. Methods and materials

2.1. Animals

Age-matched (3 months, $n = 4$) WT and D2 KO mice on the C57Bl/6J background were provided with free access to water and a standard chow diet. Mice were housed in a 10 h dark/14 h light cycle.

2.2. Immunofluorescence microscopy

Mice were perfused with 10 ml 1% fresh paraformaldehyde in phosphate buffered saline (PBS) by direct injection into the left ventricle. Epididymal fat pads were dissected and placed into 1% paraformaldehyde for 10 min at room temperature. The tissue was washed in three changes of PBS for 10 min each and cut into the desired number of samples, approximately finger-nail sized. Each sample was put into a 2 ml tube and blocked in 500 μl 5% bovine serum albumin (BSA) in PBS for 1 h. Samples were incubated in 500 μl of anti-D2 antibody dilution in 5% BSA in PBS for 2–3 h at room temperature. Samples were washed in three changes of PBS for 10 min each. Samples were then incubated in 500 μl of fluorescent conjugated secondary antibody dilution in 5% BSA in PBS for 45–60 min at room temperature. Samples were washed in three changes of PBS for 10 min each and placed in chamber mounted on #1.0 borosilicate coverglasses (Lab-Tek, catalog #155383). Samples were covered with ~150 μl Vectashield mounting medium. Images were taken using an inverted standard fluorescence or confocal microscope. All animal procedures were performed with the approval of the Institutional Animal Care and Use Committee.

2.3. Peroxisome isolation

Peroxisomes were isolated based on the protocol used for liver peroxisome preparation [11]. Mouse adipose tissue was dissected freshly and homogenized using Potter–Elvehjem homogenizer for 5 strokes in ice-cold SEM buffer (250 mM sucrose, 1 mM EDTA, 50 mM MOPS, pH 7.4). The homogenate was centrifuged at 750×*g* for 10 min to generate PNS. The PNS fraction was then centrifuged at 8500×*g* for 10 min to generate HMt. The resulting HMS was then centrifuged at 27,000×*g* for 20 min to generate LMt. The resulting LMS was centrifuged at 100,000×*g*, for 45 min to precipitate all the membrane proteins. All centrifugation was done at 4 °C. Generated fractions were resuspended in protein sample buffer (PSB, 30 mM Tris base, 10 mM EDTA, pH 6.8, 3% SDS, 20% glycerol and 0.00625% bromphenol blue) and the protein concentration determined.

2.4. Protein sample preparation and immunoblotting

Protein samples in PSB were added with 2% 2-mercaptoethanol and heated to 95 °C for 5 min before loading. Proteins were size-fractionated on 10% SDS–polyacrylamide gels and transferred to nitrocellulose membranes. Membranes were incubated in buffer A (20 mM Tris, 137 mM NaCl, 0.2% Tween 20 and 5% non-fat milk, pH 7.6) for 30 min at room temperature. Primary antibodies were diluted in buffer A and incubated with membranes for 60 min at room temperature. Membranes were washed 3 times for 5 min in buffer B (20 mM Tris, 137 mM NaCl and 0.2% Tween 20, pH 7.6). Horseradish peroxidase-conjugated secondary antibodies were diluted in buffer B and incubated with membranes for 45 min at room temperature. Membranes were washed 3 times for 5 min in buffer B and visualized by enhanced chemiluminescence (Super-Signal West Pico, Thermo Scientific).

2.5. Electron microscopy

The biochemically generated LMt fraction was fixed in 4% paraformaldehyde and washed 3 times for 5 min with 0.1 M cacodylate buffer. Samples were dehydrated in a series of graded ethanol (70% to absolute) and embedded in Epoxy resin. Ultrathin sections were inspected after contrasting with electron microscope.

WT and D2 KO mice were anaesthetized by intraperitoneal injection and perfused via the left ventricle with a mixture of 4% paraformaldehyde, 2% glutaraldehyde in 0.01 M cacodylate buffer (pH7.4). Fixed adipose tissue were dissected, cut in slices with razor blades, post-fixed in 0.5%, 1%, or 2% glutaraldehyde in cacodylate buffer (pH7.4) for 45 min, and washed 3 times for 5 min with 0.1 M cacodylate buffer. Fixed adipose tissue was embedded into LR White resin (medium grade). LR White-filled gelatin capsules were polymerized at 50 °C for 3 days. After preparation of semithin section blocks, ultrathin sections of 80 nm were cut, collected on 100-mesh nickel grids, and coated on the back side with a 1% formvar film. The grids were dried at 37 °C overnight prior to immunostaining. The sections were incubated with blocking solution (1% BSA in TBST) for 30 min at room temperature. Incubation with the primary antibodies was performed on droplets with antibodies (anti-D2 and anti-pex19) in 0.5% BSA in TBST overnight at room temperature. The sections were then incubated with secondary antibodies conjugated with gold particles (12 nm particles conjugated with anti-rabbit antibody and 6 nm particles conjugated with anti-mouse antibody) in 0.5% BSA in TBST for 1 h at room temperature. Negative controls were processed in parallel. The grids were rinsed with TBST droplets and contrasted with uranyl acetate for 2 min and lead citrate for 45 s. The sections were examined using electron microscope.

2.6. Immunoisolation of ABCD2-containing compartment and shotgun proteomics

Adipose tissue freshly collected from WT and KO mice was homogenized in ice-cold SEM buffer. Homogenates were centrifuged at 750×*g* for 10 min in 4 °C to generate PNS. Anti-D2 antibodies were biotinylated (EZ-Link™ Sulfo-NHS-LC-Biotinylation Kit, Thermo Scientific, prod #21435) and incubated with streptavidin iron beads (MagnaBind™ Streptavidin Beads, Thermo Scientific, prod #21344) for 30 min in room temperature to prepare antibody-bead complex. The complex was mixed with freshly prepared adipose PNS in 4 °C overnight for antigen–antibody binding. The mixture was put under a magnetic field to isolate the antigen–antibody-bead complexes from other components. The complex was washed sequentially with SEM buffer, triton lysis buffer (80 mM NaCl, 50 mM Tris pH8.0, 2 mM $CaCl_2$, and 1% Triton), triton lysis buffer with 0.5% SDS on ice, and triton lysis buffer with 0.5% SDS in 37 °C. Each eluate was saved and analyzed with Western blotting. For proteomic samples, only elution with triton lysis buffer with 0.5% SDS at 37 °C was applied. Eluates were enriched on a SDS–PAGE gel and processed for proteomic analysis.

The protein sample was digested with trypsin and the tryptic peptides were analyzed by LC–MS/MS using an LTQ Velos Orbitrap mass spectrometer (Thermo Fisher Scientific, Waltham, MA) coupled with a Nano-LC Ultra/cHiPLC-nanoflex HPLC system (Eksigent, Dublin, CA) through a nano-electrospray ionization source [12].

Tandem MS/MS data were acquired using CID fragmentation of selected peptides during the information-dependent acquisition. The LC–MS/MS results were subjected to protein identification and acetylation sites determination using ProteomeDiscoverer 1.3 software (Thermo Fisher Scientific, Waltham, MA) and MASCOT server.

3. Results

3.1. Immunofluorescent microscopy of ABCD2 protein in mouse adipose tissue

To determine the distribution pattern of D2 within the adipose tissue and in adipocytes in vivo, we localized D2 in adipose tissue explants by indirect immunofluorescence microscopy (Fig. 1). D2 antibody labeled the thin, cytoplasmic space, separating the lipid droplet from the cell surface (Fig. 1B). Three-dimensional reconstruction of high-magnification confocal images revealed a punctate staining pattern dispersed around the lipid droplet (Fig. 1C and D).

3.2. Localization of D2 and selected peroxisome markers in mouse adipose peroxisome preparations

To determine the subcellular localization of D2 protein within the adipocytes, mouse adipose tissue was fractionated using a procedure previously published for the isolation of peroxisomes from liver (Fig. 2A) [11]. Mouse adipose tissue was dissected and homogenized in detergent-free buffer. Sequential centrifugation was used to generate the following fractions: nuclear pellet (NP), post-nuclear supernatant (PNS), heavy mitochondria pellet (HMt), heavy mitochondria supernatant (HMS), light mitochondria pellet (LMt), light mitochondria supernatant (LMS), light membranes (LMbn), and cytosol (Cyto). Each fraction was analyzed by Western blotting to determine the relative abundance of D2 and selected peroxisome markers in each fraction (Fig. 2B). D2, catalase, D3 (a.k.a PMP70), and PEX19 were all present in the PNS and HMS fractions. However, D2 fractionated with LMt (27,000 g), while catalase, PEX19 and D3 remained in suspension (LMS) and sequentially precipitated LMbns (100,000 g). Liver peroxisomes generally co-fractionate with LMt and are subsequently separated on a continuous sucrose gradient. However,

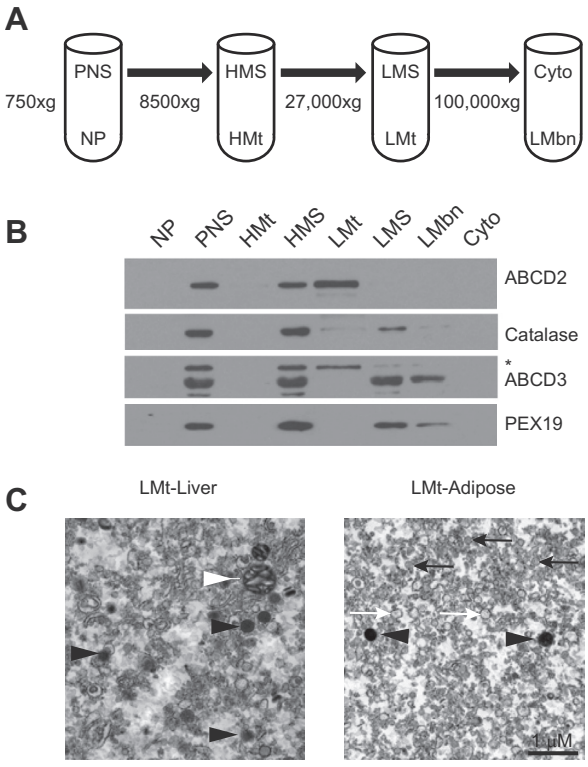

Fig. 2. Abundance of D2 and other peroxisome markers in biochemically generated fractions from adipose tissue. (A) Mouse adipose tissue was homogenized in SEM buffer and sequentially centrifuged to separate subcellular fractions. (B) 2.3% of each fraction was analyzed for the abundance of D2 and other peroxisome marker proteins by Western blotting. The asterisk indicates residual signal of D2 from prior blotting. (C) LMt from liver and adipose tissues were fixed in 4% paraformaldehyde and imaged using electron microscopy. Mitochondria, and peroxisomes are indicated by white, and black arrowheads. Spherical vesicles with transparent lumen or dense matrix are indicated by white or black arrows.

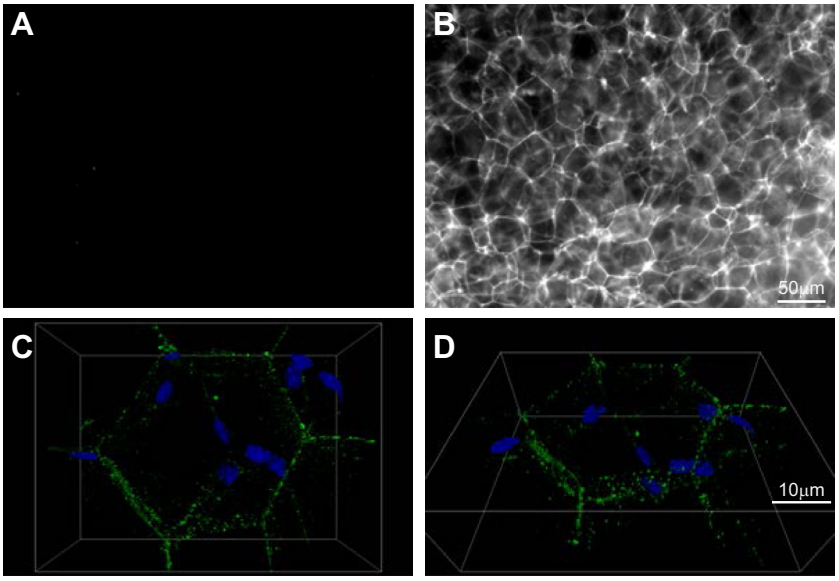

Fig. 1. Immunolocalization of D2 in mouse adipose tissue explants. Mouse epididymal fat pads were fixed with 1% paraformaldehyde and processed for indirect immunofluorescence microscopy. (A and B) Low power (10×) images of fixed adipose explants labeled with either pre-immune serum (A) or anti-D2 polyclonal antibody (B). (C and D) Three dimensional reconstruction of 60 (0.6 mm/slice) high power, confocal images (63×) with 0o (C) or 45o rotation (D) along the *z*-axis. Green color denotes D2 labeled with AlexaFluor 488. Blue denotes nuclei stained with DAPI. (For interpretation of the references to color in this figure legend, the reader is referred to the web version of this article.)

most peroxisome markers in adipose remained suspended and only D2 came down in the LMt. This is unlikely due to peroxisome rupture since these markers include D3, a protein with multiple membrane spanning segments and that other markers pelleted at 100,000 g.

Next, we fixed the LMt pellets from both liver and adipose tissue and processed them for electron microscopy (Fig. 2C). We used liver as a positive control to see evidence of both mitochondria (white arrow) and peroxisomes (black arrows) with their characteristic dense matrix and ~0.2 μm diameter. LMt pellets from adipose also revealed mitochondria, but in fewer numbers, as well as structures with the typical appearance of peroxisomes. However, the fraction was highly enriched with ~0.1 μm diameter spherical structures with clearly defined membranes (white and black arrows). Some contained evidence of a matrix (black arrows), but were not as electron dense as typical liver peroxisomes. With the separation of D2 from catalase and PEX19, we hypothesized that D2 may be localized in a subclass of peroxisome in adipocytes.

3.3. Localization of D2 and PEX19 in fixed mouse adipose tissues

Next, we prepared an LMt fraction from both wild-type (WT) and D2 knock-out (KO) adipose tissues. The fractions were fixed and immunostained with D2 antibody and detected by secondary antibody cross-linked with gold particles (6 nm diameter, Fig. 3A). In the WT sample, the D2 antibody specifically labeled the compartments (white arrows) with a more electron dense center as distinct from the surrounding vesicular structures. The same compartments were present in the KO sample, but not labeled with D2 antibody.

To determine if the D2 compartment was distinct from the PEX19 compartment in vivo, we fixed mouse epididymal adipose explants, cut them into ultrathin sections of 80 nm, and immunostained them with the D2 and PEX19 antibodies. D2 (white arrows) and PEX19 (black arrow) were detected with secondary antibodies linked with 6 nm and 12 nm gold particles, respectively (Fig. 3B). PEX19 and D2 antibodies recognized distinct structures and did not exhibit overlap in adipose sections.

3.4. Immunoisolation and proteomic profiling of the D2-containing compartment

We next sought to characterize the proteome of the D2-containing compartment. We cross-linked our D2 antibody to biotin and used it to immunoisolate D2-containing organelles from mouse adipose homogenates using avidin-coated magnetic beads. The immunoisolated compartment was eluted sequentially with buffers containing Triton-X 100, Triton-X 100 plus 0.5% SDS at 4 °C

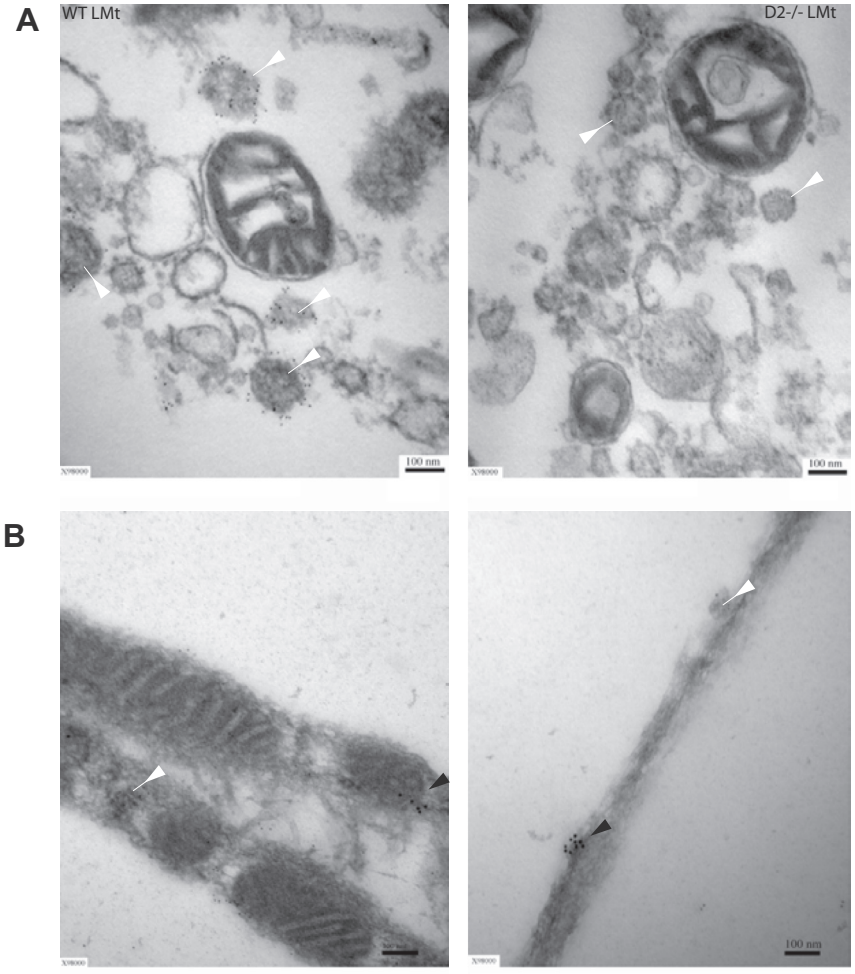

Fig. 3. Localization of D2 and PEX19 in fixed mouse adipose tissue. (A) LMt were prepared using freshly collected adipose tissue from WT and D2 KO mice by sequential centrifugation. The LMt fractions were fixed in 4% paraformaldehyde and embedded in Epoxy resin. Ultrathin sections were cut and immunostained using D2 antibody and secondary antibody (cross-linked with 6 nm diameter gold particles). Peroxisome-like compartments are indicated by white arrowheads. (B) Fixed epididymal fat was cut into ultrathin sections of 80 nm, immunostained with D2 antibody and secondary antibody (cross-linked with 6 nm gold particles, indicated by empty arrowheads) and PEX19 antibody and secondary antibody (cross-linked with 12 nm gold particles, indicated by black arrowheads).

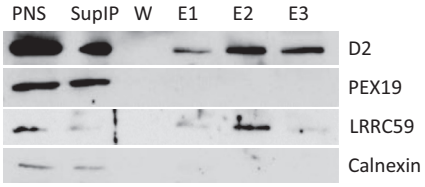

Fig. 4. Immunoisolation of the D2-containing compartment. D2 antibody captured compartment was isolated from the supernatant (SupIP) under the magnetic field and sequentially washed by SEM buffer on ice (W), triton lysis buffer on ice (E1), triton lysis buffer + 0.5% SDS on ice (E2) and triton lysis buffer + 0.5% SDS under 37 °C (E3). Each fraction was analyzed for abundance of D2, PEX19, LRRC59 and calnexin using Western blotting.

and the same buffer at 37 °C. Eluted fractions were processed by SDS–PAGE and analyzed by Western blotting (Fig. 4). D2 was detected in the starting material (PNS) as well as the supernatant (SupIP) after immunocapture, but in a much reduced amount. A modest amount of D2 was eluted with Triton alone (E1). Solubilization of D2 required the addition of SDS in the elution buffer (E2 and E3) and beads. Boiling in SDS under reducing conditions released a small amount of residual D2 from the magnetic beads (data not shown). As in the centrifugation approach, PEX19 did not co-elute with D2. Calnexin was blotted as a negative control for bulk ER proteins.

Thereafter, we applied shotgun proteomics to analyze the D2-containing organelles from independently prepared WT ($n = 4$) and KO ($n = 3$) adipose tissues. To concentrate proteins in the D2 compartment, we directly eluted in buffer E3 following the wash step. Eluates were subjected to mass spectrometry analysis to obtain the D2 associated proteome from adipose. Any peptides present in KO samples were considered non-specific associations. Uniprot IDs of proteins identified exclusively in the WT samples were analyzed by the DAVID functional annotation tool. Proteins associated with D2 were annotated peroxisomal, mitochondrial, and ER-related (Table 1).

One of the proteins with the strongest association with D2 was LRRC59, which was present in all four WT samples. Therefore, we re-probed our elution fractions for LRRC59 (Fig. 4). LRRC59 was detected in PNS and in a much reduced amount in SupIP. A modest amount of LRRC59 was present in E1 and E3, and eluted most in E2. These data support the strong association of LRRC59 with D2 in adipose peroxisomes.

Table 1
Proteins associated with the D2-containing compartment. The D2-containing compartment in adipose homogenates of WT and D2 KO mice was immunoisolated using D2 antibody-cross-linked magnetic beads in detergent free buffer. The compartment was eluted using triton lysis buffer + 0.5% SDS and subjected to mass spectrometry analysis. Proteins detected exclusively in the WT samples but absent in the KO samples are listed in this table.

Peroxisome
ATP-binding cassette, sub-family D (ALD), member 2
ATP-binding cassette, sub-family D (ALD), member 3
Carnitine acetyltransferase
Dehydrogenase/reductase (SDR family) member 7B
Enoyl coenzyme A hydratase 1, peroxisomal
Enoyl-coenzyme A, hydratase/3-hydroxyacyl coenzyme A dehydrogenase
Nephronophthisis 3 (adolescent); acyl-coenzyme A dehydrogenase family, member 11
Sterol carrier protein 2
Mitochondrion
3-oxoacid CoA transferase 1
ATP synthase, H + transporting, mitochondrial F0 complex, subunit b, isoform 1; predicted gene 12231
Cytochrome c oxidase subunit 2
NADH dehydrogenase (ubiquinone) 1 alpha subcomplex, 8
NADH dehydrogenase (ubiquinone) 1 alpha subcomplex, 9
NADH dehydrogenase (ubiquinone) flavoprotein 1
Aconitase 2, mitochondrial
Acyl-Coenzyme A dehydrogenase, medium chain
Carbonyl reductase 2
Carnitine acetyltransferase
Carnitine palmitoyltransferase 2
Citrate synthase
Cytochrome c oxidase subunit IV isoform 1
Cytochrome c oxidase, subunit VI a, polypeptide 1; predicted gene 7795
Dihydrolipoamide dehydrogenase
Enoyl coenzyme A hydratase 1, peroxisomal
Fumarate hydratase 1
Malate dehydrogenase 2, NAD (mitochondrial)
Predicted gene 6123; pyruvate dehydrogenase (lipoamide) beta
Predicted gene 6835; ATP synthase, H + transporting, mitochondrial F0 complex, subunit f, isoform 2; predicted gene 6581
Sideroflexin 1
Solute carrier family 25 (mitochondrial carrier, adenine nucleotide translocator), member 4
Ubiquinol-cytochrome c reductase, complex III subunit VII
Endoplasmic reticulum
Leucine-rich repeat-containing protein 59 OS = Mus musculus GN = Lrrc59 PE = 2 SV = 1 – [LRC59_MOUSE]
1-acylglycerol-3-phosphate O-acyltransferase 9
ATPase, Ca++ transporting, cardiac muscle, fast twitch 1
SAC1 (suppressor of actin mutations 1, homolog)-like (*S. cerevisiae*)
SEC22 vesicle trafficking protein homolog B (*S. cerevisiae*)
UDP-glucose ceramide glucosyltransferase-like 1; similar to UDP-glucose ceramide glucosyltransferase-like 1
Alpha glucosidase 2 alpha neutral subunit
Calreticulin
Dolichyl-di-phosphooligosaccharide-protein glycotransferase
Endoplasmic reticulum protein 29
Heat shock protein 90, beta (Grp94), member 1
Peptidylprolyl isomerase B
Prolyl 4-hydroxylase, beta polypeptide
Ribophorin II

4. Discussion

We have shown that D2 is localized in a subclass of peroxisomes potentially associated with mitochondria and ER in mouse adipose tissue. This is the first report that describes the subcellular localization of D2 in adipose tissues.

Our findings indicate that the D2-containing compartment harbors peroxisomal proteins, but lacks some of the well-established markers, thereby distinguishing itself as a subclass of peroxisomes in adipose. The concept of "microperoxisomes" was early proposed with evidence showing their close association with lipid droplets and ER in cultured adipocytes [4]. However, their characteristics and functions in adipose tissue remained undescribed. In recent years, interest is reemerging in these organelles with the discovery that peroxisome dysfunction leads to several adipose phenotypes [5,6]. These findings are generally obtained from peroxin-deficient mouse models in which peroxisomal membrane protein assembly is disrupted. Additionally, peroxisomes were not further categorized and no attempt was made to assess tissue-specific effects of peroxisome dysfunction. Our results suggest the existence of distinct subclasses of peroxisomes within adipose, suggesting that even within a given tissue peroxisome function may be differentially affected.

D2 has been shown to play essential roles in lipid metabolism [7–9]. Although D2 is not highly expressed in tissues characterized with high rates of β-oxidation, it is highly abundant in white adipose tissue [8]. Given that white adipose is far less metabolically active and contains fewer peroxisomes, the need for such high levels of D2 in adipose is unclear. D2 has been shown to be critical for erucic acid catabolism [9]. However, erucic acid is present in trace amounts in most plant and seed oils, suggesting other essential functions of D2 in endobiotic and xenobiotic metabolism [9]. Given the distinct substrate specificities of peroxisomal transporters, the

D2-compartment may differ from other peroxisomes in substrate access.

Our findings suggest a close relationship between D2-containing peroxisomes and mitochondria and ER. Using an immunoisolation approach combined with mass spectrometry, we purified a D2 containing compartments from adipose tissue and determined its proteomic profile. Besides peroxisomal proteins, we also identified mitochondrial and ER proteins. This is consistent with emerging evidence indicating that peroxisomes, mitochondria, and ER may be physically associated with each other [13]. The movement of peroxisomes is coupled with mitochondria, independent of cytoskeleton during cell division in yeast [14]. Peroxisomes also derive a portion of their components from mitochondria through a vesicular transport pathway [15]. The physiological function of this pathway is still unknown, but might involve the transport of both lipid metabolites and proteins.

There is also growing evidence suggesting that peroxisomes may form out of ER in a "budding" pattern and derive some of their proteins and membranes through this mechanism [13]. Vesicles originating from ER were shown to be routed to peroxisomes with the assistance of Pex16 or Pex3 and the ER budding factor Sec16b in human fibroblasts [16–18]. These vesicular structures were referred as "preperoxisomes," and two biochemically distinct populations have been identified [13]. Preperoxisomes must fuse with other more mature peroxisomes to generate functional organelles [13]. Therefore, there are at least four subpopulations of peroxisomes present within a cell: the two distinct preperoxisomes, the more mature, but not fully functional peroxisomes, and the fully mature and functional peroxisomes. The D2-containing peroxisome in adipose may be categorized into one of the first three subgroups or even distinguish itself as another subclass of peroxisomes unique to adipocytes.

Finally, we observed that the putative trafficking protein, LRRC59, is closely associated with D2-containing compartment. The biological function of LRRC59 is still poorly understood. A recent report indicates the interaction of LRRC59 with Selenoprotein S (SelS), an ER protein involved in the protein retro-translocation from ER to cytosol and the inflammatory response, however, the influence of LRRC59 on SelfS functions was not investigated [19]. Nonetheless, their interaction indicates a potential role of LRRC59 in the trafficking of vesicles originating from the ER. The interaction of LRRC59 and D2 suggests the possible origin of some components of the D2-conatining peroxisome from the ER. Another group reported that LRRC59 facilitates the intracellular trafficking of fibroblast growth factor 1 (FGF1) into nucleus in cultured cells [10]. Given the importance of FGF1-PPARγ signaling axis in adipocyte metabolism, LRRC59 may be essential for normal adipose functions [20]. Its association with D2 may potentially bridge D2 dependent lipid metabolism and FGF1 signaling in adipose tissue.

Acknowledgments

This work was funded by grants from the National Institute of Diabetes and Digestive and Kidney Diseases (Grant DK080874, DK100892). The content is solely the responsibility of the authors and does not necessarily represent the official views of the National Institutes of Health. We acknowledge the University of Kentucky Proteomics Core that is partially supported by grants from the National Cancer Institute (P30CA177558) and the National Institute of General Medical Sciences (P20GM103486) from the National Institutes of Health. The authors would like to acknowledge Jeannie Haak for assistance with manuscript preparation.

References

[1] J. Rhodin, Electron microscopy of the kidney, Am. J. Med. 24 (1958) 661–675.
[2] I.J. Lodhi, C.F. Semenkovich, Peroxisomes: a nexus for lipid metabolism and cellular signaling, Cell Metab. 19 (2014) 380–392.
[3] P.P. Van Veldhoven, M. Baes, Peroxisome deficient invertebrate and vertebrate animal models, Front. Physiol. 4 (2013) 335.
[4] A.B. Novikoff, P.M. Novikoff, O.M. Rosen, C.S. Rubin, Organelle relationships in cultured 3T3-L1 preadipocytes, J. Cell Biol. 87 (1980) 180–196.
[5] K. Martens, A. Bottelbergs, A. Peeters, F. Jacobs, M. Espeel, P. Carmeliet, P.P. Van Veldhoven, M. Baes, Peroxisome deficient aP2-Pex5 knockout mice display impaired white adipocyte and muscle function concomitant with reduced adrenergic tone, Mol. Genet. Metab. 107 (2012) 735–747.
[6] P. Brites, A.S. Ferreira, T.F. da Silva, V.F. Sousa, A.R. Malheiro, M. Duran, H.R. Waterham, M. Baes, R.J. Wanders, Alkyl-glycerol rescues plasmalogen levels and pathology of ether-phospholipid deficient mice, PLoS One 6 (2011) e28539.
[7] M. Morita, T. Imanaka, Peroxisomal ABC transporters: structure, function and role in disease, Biochim. Biophys. Acta 2012 (1822) 1387–1396.
[8] J. Liu, N.S. Sabeva, S. Bhatnagar, X.A. Li, A. Pujol, G.A. Graf, ABCD2 is abundant in adipose tissue and opposes the accumulation of dietary erucic acid (C22:1) in fat, J. Lipid Res. 51 (2010) 162–168.
[9] J. Liu, S. Liang, X. Liu, J.A. Brown, K.E. Newman, M. Sunkara, A.J. Morris, S. Bhatnagar, X. Li, A. Pujol, G.A. Graf, The absence of ABCD2 sensitizes mice to disruptions in lipid metabolism by dietary erucic acid, J. Lipid Res. 53 (2012) 1071–1079.
[10] Y. Zhen, V. Sorensen, C.S. Skjerpen, E.M. Haugsten, Y. Jin, S. Walchli, S. Olsnes, A. Wiedlocha, Nuclear import of exogenous FGF1 requires the ER-protein LRRC59 and the importins Kpnalpha1 and Kpnbeta1, Traffic 13 (2012) 650–664.
[11] J.M. Graham, Isolation of peroxisomes from tissues and cells by differential and density gradient centrifugation, Curr. Protoc. Cell Biol. (2001) (Chapter 3, Unit 3 5).
[12] X. Li, Q. Zhou, M. Sunkara, M.L. Kutys, Z. Wu, P. Rychahou, A.J. Morris, H. Zhu, B.M. Evers, C. Huang, Ubiquitylation of phosphatidylinositol 4-phosphate 5-kinase type I gamma by HECTD1 regulates focal adhesion dynamics and cell migration, J. Cell Sci. 126 (2013) 2617–2628.
[13] A. van der Zand, J. Gent, I. Braakman, H.F. Tabak, Biochemically distinct vesicles from the endoplasmic reticulum fuse to form peroxisomes, Cell 149 (2012) 397–409.
[14] I. Jourdain, D. Sontam, C. Johnson, C. Dillies, J.S. Hyams, Dynamin-dependent biogenesis, cell cycle regulation and mitochondrial association of peroxisomes in fission yeast, Traffic 9 (2008) 353–365.
[15] M. Neuspiel, A.C. Schauss, E. Braschi, R. Zunino, P. Rippstein, R.A. Rachubinski, M.A. Andrade-Navarro, H.M. McBride, Cargo-selected transport from the mitochondria to peroxisomes is mediated by vesicular carriers, Curr. Biol. 18 (2008) 102–108.
[16] P.K. Kim, R.T. Mullen, U. Schumann, J. Lippincott-Schwartz, The origin and maintenance of mammalian peroxisomes involves a de novo PEX16-dependent pathway from the ER, J. Cell Biol. 173 (2006) 521–532.
[17] A.A. Toro, C.A. Araya, G.J. Cordova, C.A. Arredondo, H.G. Cardenas, R.E. Moreno, A. Venegas, C.S. Koenig, J. Cancino, A. Gonzalez, M.J. Santos, Pex3p-dependent peroxisomal biogenesis initiates in the endoplasmic reticulum of human fibroblasts, J. Cell. Biochem. 107 (2009) 1083–1096.
[18] S. Yonekawa, A. Furuno, T. Baba, Y. Fujiki, Y. Ogasawara, A. Yamamoto, M. Tagaya, K. Tani, Sec16B is involved in the endoplasmic reticulum export of the peroxisomal membrane biogenesis factor peroxin 16 (Pex16) in mammalian cells, Proc. Natl. Acad. Sci. USA 108 (2011) 12746–12751.
[19] A.A. Turanov, V.A. Shchedrina, R.A. Everley, A.V. Lobanov, S.H. Yim, S.M. Marino, S.P. Gygi, D.L. Hatfield, V.N. Gladyshev, Selenoprotein S is involved in maintenance and transport of multiprotein complexes, Biochem. J. (2014).
[20] J.W. Jonker, J.M. Suh, A.R. Atkins, M. Ahmadian, P. Li, J. Whyte, M. He, H. Juguilon, Y.Q. Yin, C.T. Phillips, R.T. Yu, J.M. Olefsky, R.R. Henry, M. Downes, R.M. Evans, A PPARgamma-FGF1 axis is required for adaptive adipose remodelling and metabolic homeostasis, Nature 485 (2012) 391–394.